Ion Yields in the Coupled Chemical and Physical Dynamics Model of Matrix-Assisted Laser Desorption/Ionization

Richard Knochenmuss

Published as J. Am. Soc. Mass Spectrom. (2015) 26:1645-1648
DOI 10.1007/s13361-015-1225-8

Abstract

The Coupled Chemical and Physical Dynamics (CPCD) model of matrix assisted laser desoprtion ionization has been restricted to relative rather than absolute yield comparisons because the rate constant for one step in the model was not accurately known. Recent measurements are used to constrain this constant, leading to good agreement with experimental yield vs fluence data for 2,5 dihydroxybenzoic acid. Parameters for alpha-cyano-4-hydroxycinnamic acid are also estimated, including contributions from a possible triplet state.The results are compared to the polar fluid model, the CPCD is found to give better agreement with the data.

Introduction

Both thermal and non-thermal primary ionization mechanisms have been proposed for ultraviolet MALDI, see [1] for a review. The simplest thermal model is perhaps the Polar Fluid Model (PFM),[2, 3] which was recently revived and cast into quantitative form by the Ni group.[4] Similar proposals have been made by the Kim group.[5, 6] In the PFM, liquid matrix acts as a solvent to promote autoprotolysis of the matrix itself to form ion pairs. It is assumed that this reaction proceeds to equilibrium, and that the matrix fluid is a good solvent for ions. Several assumptions of the PFM have recently been challenged.[7]

In the Coupled Chemical and Physical Dynamics (CPCD) model proposed by the author, mobile electronic excitations (excitons) play a key role. Pooling reactions of these excitons allows sufficient concentration of energy for initial charge separation. A detailed, quantitative model has been constructed for 2,5 dihydroxybenzoic acid (DHB) and other matrixes, in which the photochemistry and ablation physics are modeled as a function of time.[8-12] The key steps in ion formation are:

$S_0 + h\upsilon \rightarrow S_1$ Matrix photoexcitation

$S_1 + S_1 \rightarrow S_n + S_0$ Pooling of two excitons

$S_n + S_1 \rightarrow M^+ + e^- + S_0$ Pooling of two excitons, including one higher excited state.

The electron is captured within about 10 nm to form a matrix anion. Matrix radical ions react rapidly to form protonated/deprotonated ion pairs, which engage in secondary reactions with analyte. The model may include intersystem crossing (ISC) and reaction of triplet excitons. As was recently shown for 2,4,6 trihydroxyacetophenone (THAP) matrix, ISC may be quite efficient in some MALDI matrices.[13]

The CPCD has successfully reproduced a number of MALDI phenomena related to both primary and secondary ionization.[1, 10, 14-16, 16, 16, 17, 17-24] However, these were restricted to comparisons which do not depend on absolute ion yields (relative intensities, for example) since both experimental yields and the rate constant for the last step in the ion formation process above were poorly known.

The Ni group has recently reported new attempts to measure absolute ion yields (ion number/neutral number).[25] They conclude that these are in the 10^{-9} to 10^{-8} range for DHB, sinapinic acid and ferulic acid, and in the 10^{-8} to 10^{-7} range for alpha-cyano-4-hydroxycinnamic acid (CHCA), with standard errors of about an order of magnitude. These and earlier values were used to argue that the CPCD cannot be correct because it is claimed to predict yields which are too high.[4, 26-28] Here we use the newest data to revise the $S_n + S_1$ pooling rate constants, and to test the revised model against the data for DHB and CHCA matrices.

Methods

The rate equation implementation of the CPCD[8-10] was used. The set of equations was implemented in the Igor Pro environment (Wavemetrics, Lake Oswego, OR, USA), and numerically integrated using double-precision, 5th-order Runge Kutta methods, with adaptive step size. Mass balance was checked throughout the integration, the maximum error was typically less than 10^{-14}.

A temporally gaussian 355 nm laser pulse with 5 ns width was used. The vaporization temperature was taken to be 400 K for DHB and 450 K for CHCA. The sample is modeled as a stack of layers, with the thicknesses adjusted for constant absorbed laser energy. The results for the layers are summed. Diffusion and mixing of layers is taken to be negligible, since layers nearer the surface are ejected with higher velocity than deeper ones. The matrix parameters were initially taken from earlier studies, particularly the wavelength and fluence study of ref. [17].

Results and Discussion

DHB is the matrix for which the CPCD was originally developed. Singlet exciton pooling in DHB has been repeatedly investigated[29-32] and is the key process bringing together energy for charge separation in the CPCD. Using the original estimated rate constant for the $S_n + S_1$ pooling step, 10^9 s^{-1}, the CPCD predicts that absolute yields vs fluence are in the range of 10^{-4}, as seen in Fig. 1, top trace.

The $S_n + S_1$ pooling rate constant was reduced to 10^8 s^{-1} in the middle trace. The form of the curve remains virtually identical, there is only a vertical shift. Note that there is also no change in the ion appearance threshold, at 10 mJ/cm^2. The threshold is an ablation effect, not due to ion formation. If the material does not ablate, ions can not be released. Charge separation does occur at fluences too low for ablation, as evidenced by electron emission.[33] Some electrons escape the solid matrix due to their relatively long mean free path. The phase change temperature for the upper two traces in Fig. 1 was 450 K, as used previously.

In the lowest CPCD model trace, the $S_n + S_1$ pooling rate constant was $3x10^6$ s^{-1} and the phase change temperature was decreased to 400 K. The latter shifted the appearance threshold to 7 mJ/cm^2, and the former was chosen for best agreement with the data of Lu et al.,[25] which is also shown in the figure. Agreement between model and data is essentially exact at all fluences above the threshold.

Also shown in Fig. 1 is the yield prediction of the PFM as implemented by Ni. Only the high temperature curve is shown. Use of the low temperature g factor in a high temperature ablation event is considered inappropriate, and the high temperature curve is anyway a better fit to the data. The PFM prediction crosses the data, but is an order of magnitude in error on both ends. On the high fluence end it is rising with about double the slope (in the logarithmic plot) as the data and CPCD.

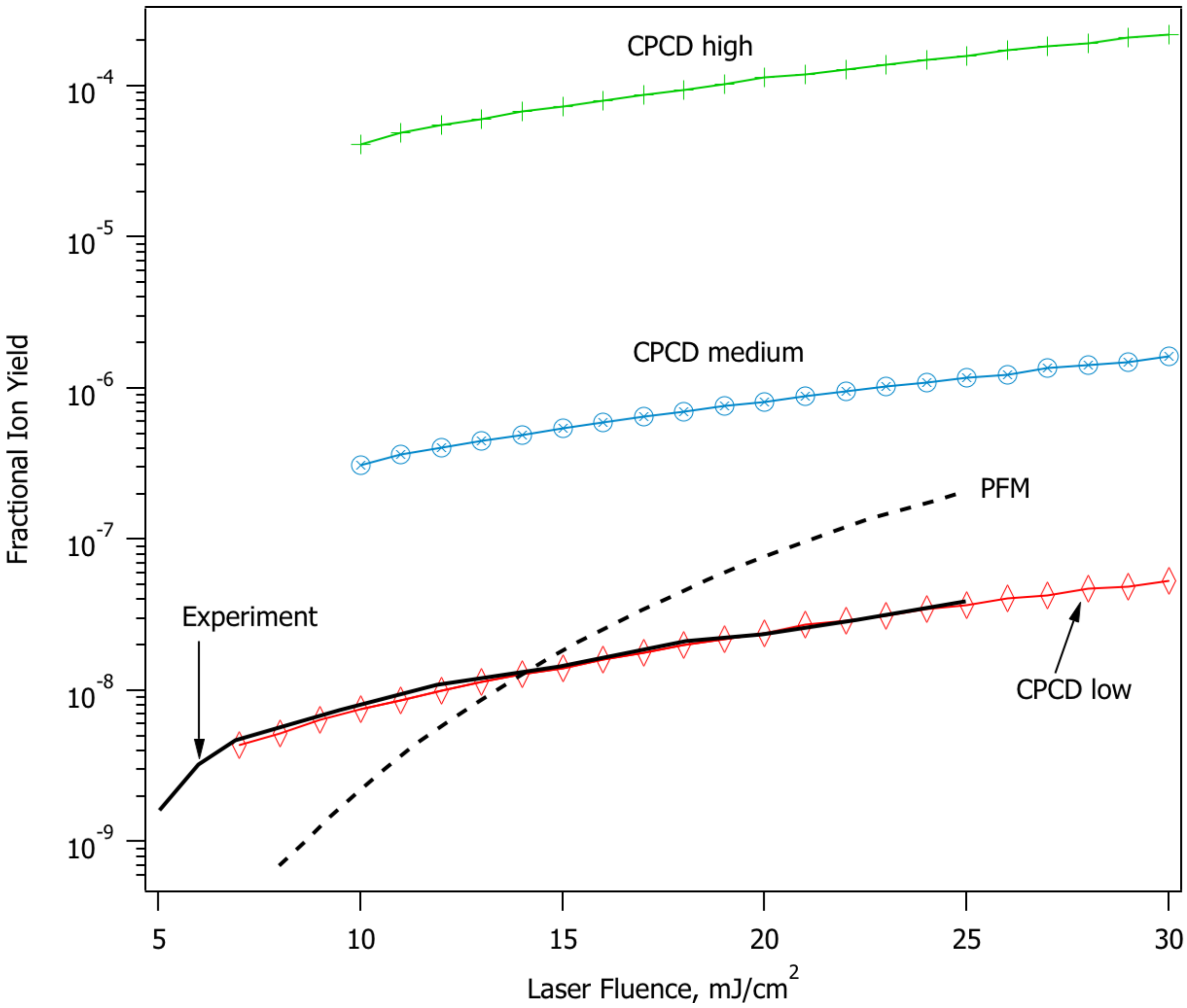

Figure 1. CPCD yield curves for DHB matrix. High and low refer to the $S_n + S_1$ pooling rate constants, see the text for details. The experimental fit curve and PFM predictions are from [25]. The experimental standard errors are an order of magnitude or more.

The matrix CHCA is more complicated than DHB,[30, 34] though it also has been successfully modeled with the CPCD.[17] At least two emitting excited states, and photoinduced reaction, possibly dimerization, have been proposed.[30] Even more extensive photoreaction has been proposed for sinapinic acid, with long-lived products.[30] This implies that the PFM predictions of matrix fluid solvation properties are incorrect, since during and after laser irradiation the material is chemically altered.

Fig. 2 shows the CPCD prediction for CHCA matrix, with the S_n + S_1 pooling rate constant reduced to 10^7 s^{-1} from $2x10^9$ s^{-1}, indicated by round symbols. This curve represents the same model as for DHB, only singlet excited states and only singlet pooling reactions are included. This is expected to be too simple, and this result seems to confirm that. Nevertheless, the CPCD curve is still a better fit than the PFM model, at all fluences above the "knee," or change in curvature in the experimental data.

The CPCD has been extended to include triplet states, as part of the investigation of THAP matrix.[13] That formalism was used here as a means to include an approximation to the additional excited states or species that are relevant for CHCA. Since only a single excitation wavelength is considered here, this is feasible, obviating the need to characterize species with differing absorption spectra.[17]

The trace with diamond symbols includes intersystem crossing (ISC) to a triplet with a lifetime of 1.5 ns, in addition to the singlet processes. The singlet lifetime was also reduced to 35 ps, consistent with photophysical data.[30] The ISC rate of 10^9 s^{-1} is similar to THAP. Some triplet pooling is included for improved agreement with experiment ($3T_1 \rightarrow S_0 + M^+ + M^-$, rate constant=$5x10^7$ s^{-1}). The triplet stores electronic energy longer than the S_1, and converts it mostly to heat. At low fluence, triplet energy storage reduces yield, but at higher fluences singlet ionization pathways become more efficient, and the curve flattens toward the singlet-only result.

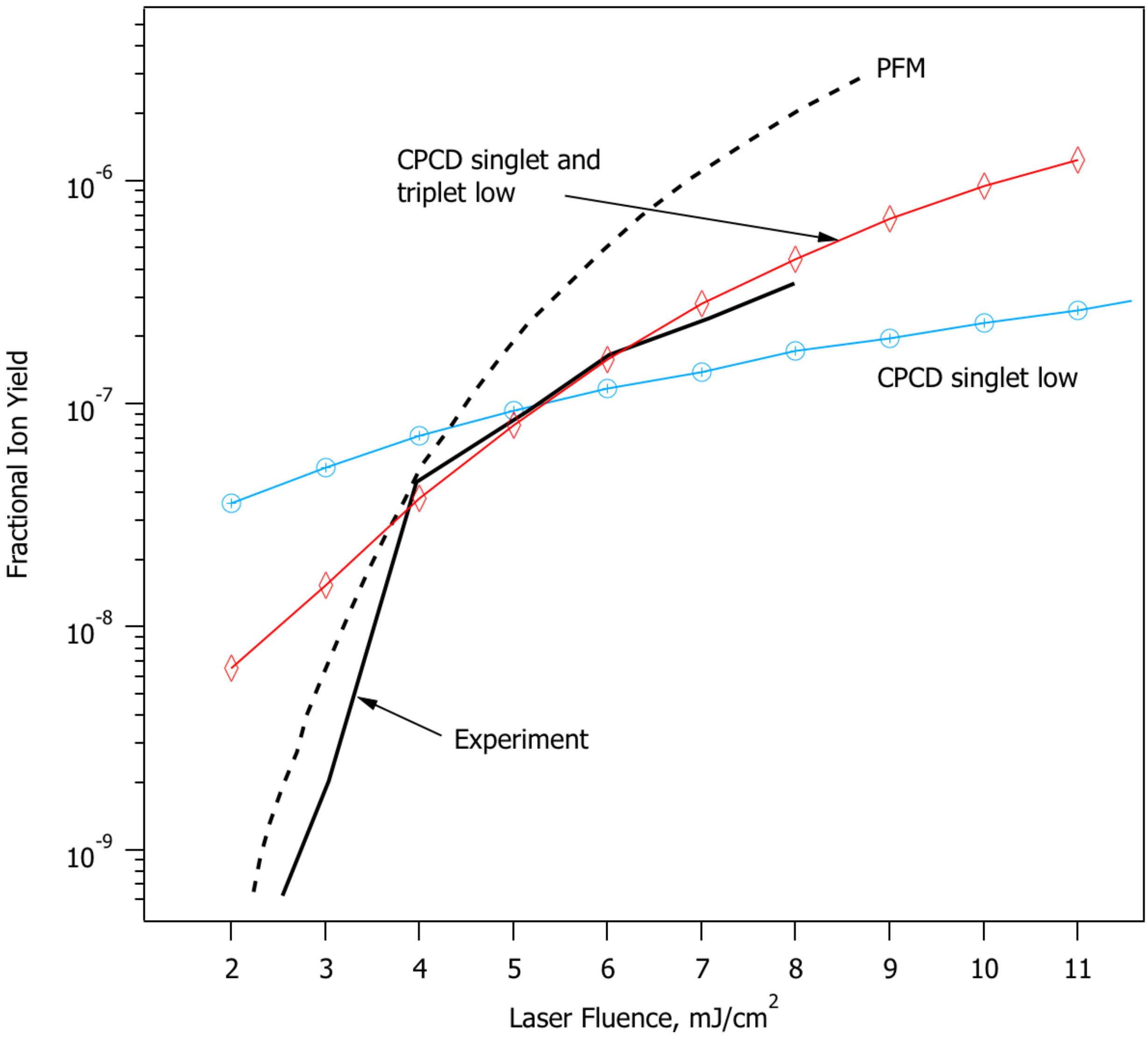

Figure 2. CPCD yield curves for CHCA matrix, see the text for details. The experimental fit curve and PFM predictions are from [25]. The experimental standard errors are an order of magnitude or more.

Both the DHB and CHCA yield data show a distinct drop at the lowest fluences, large in CHCA, small in DHB. The origin of the "knee" in the curves is unclear, it is not currently predicted by any model. Since it occurs at the lowest fluences, it must involve material that ablates easily, at a low temperature. The CPCD model suggests that this would have to be at less than 400 K in the DHB case, not far above room temperature. A material that would readily ablate at low temperature would presumably not survive the pumpdown to MALDI pressures. This suggests that it may represent low molecular weight photochemical products of the original matrix material, rather than simple contaminants. Since not all of this material would necessarily vaporize during the ablation event that created it, some will be present for the next shot, changing the characteristic of subsequent ablation events. This is consistent with the data on CHCA and sinapinic acid,[30] and with the need to model two absorbing species.[17] It becomes most apparent at low fluence, when not overshadowed by the original matrix material.

Conclusions

As noted in earlier CPCD studies,[17] the model can be readily adapted to a range of absolute MALDI ion yields by variation of otherwise poorly known or unconstrained parameters, particularly the $S_n + S_1$ pooling rate. So adapted, the CPCD is found to be in excellent agreement with the data of Lu et al.[25] for DHB. Relative trends are affected very little by this rate, which is why earlier such comparisons were consistent with experiment.

The matrix CHCA can also be well modeled by the CPCD, if a second excited state is included, consistent with earlier studies of CHCA. Agreement with the measured data is good, but the interpretation of the second state as a triplet remains tentative.

For both DHB and CHCA, the CPCD results correspond better with the data than the PFM predictions of Lu et al.[25], particularly at higher fluences.

In both matrices the lowest fluence data are anomalous. The observed change in curvature at low fluence is not predicted by either theory. A possible explanation could be photoproducts formed during prior laser shots.

References

1. Knochenmuss, R.: Ion formation mechanisms in UV-MALDI. *The Analyst,* **131**, 966-986 (2006)
2. Niu, S., Zhang, W., Chait, B. T.: Direct Comparison of Infrared and Ultraviolet Wavelength Matrix-Assisted Laser Desorption/Ionization Mass Spectrometry of Proteins. *J. Am. Soc. Mass Spectrom.,* **9**, 1-7 (1998)
3. Chen, X., Carroll, J. A., Beavis, R. C.: Near-Ultraviolet-Induced Matrix-Assisted Laser Desorption/Ionization as a Function of Wavelength. *J. Am. Soc. Mass Spectrom.,* **9**, 885-891 (1998)
4. Chu, K. Y., Lee, S., Tsai, M.-T., Lu, I.-C., Dyakov, Y. A., Lai, Y. H., Lee, Y.-T., Ni, C.-K.: Thermal Proton Transfer Reactions in Ultraviolet Matrix-Assisted Laser Desorption/Ionization. *J. Am. Soc. Mass Spectrom.,* 310-318 (2014)
5. Ahn, S. H., Park, K. M., Bae, Y. J., Kim, M. S.: Quantitative reproducibility of mass spectra in matrix-assisted laser desorption ionization and unraveling of the mechanism for gas-phase peptide ion formation. *J. Mass Spectrom.,* **48**, 299-305 (2013)
6. Bae, Y. J., Choe, J. C., Moon, J. H., Kim, M. S.: Why do the Abundances of Ions Generated by MALDI Look Thermally Determined? *J. Am. Soc. Mass Spectrom.,* **24**, 1807-1815 (2013)
7. Knochenmuss, R.: Energetics and Kinetics of Thermal Ionization Models of MALDI. *J. Am. Soc. Mass Spectrom.,* **25**, 1521-1527 (2014)
8. Knochenmuss, R.: A Quantitative Model of Ultraviolet Matrix-assisted Laser Desorption and Ionization. *J. Mass Spectrom.,* **37**, 867-877 (2002)
9. Knochenmuss, R.: A Quantitative Model of UV-MALDI Including Analyte Ion Generation. *Anal. Chem.,* **75**, 2199 (2003)
10. Knochenmuss, R.: A bipolar rate equation model of MALDI primary and secondary ionization processes, with application to positive/negative analyte ion rations and suppression effects. *Int. J. Mass Spectrom.,* **285**, 105-113 (2009)
11. Knochenmuss, R., Zhigilei, L. V.: A molecular dynamics model of UV-MALDI including ionization processes. *J. Phys. Chem. B,* **109**, 22947-229957 (2005)
12. Knochenmuss, R., Zhigilei, L. V.: Molecular dynamics simulations of MALDI: laser fluence and pulse width dependence of plume characteristics and consequences for matrix and analyte ionization. *J. Mass Spectrom.,* **45**, 333-346 (2010)

13. Kirmess, K. M., Knochenmuss, R., Blanchard, G. J.: Excited State Dynamics in the MALDI Matrix 2,4,6 Trihydroxyacetophenone: Evidence for Triplet Pooling Charge Separation Reactions. *Rapid Comm. Mass Spectrom.,* **28**, 2134-2140 (2014)
14. Knochenmuss, R., Dubois, F., Dale, M. J., Zenobi, R.: The Matrix Suppression Effect and Ionization Mechanisms in Matrix-Assisted Laser Desorption/Ionization. *Rapid Commun. Mass Spectrom.,* **10**, 871-877 (1996)
15. Knochenmuss, R., Karbach, V., Wiesli, U., Breuker, K., Zenobi, R.: The Matrix Suppression Effect in Matrix-Assisted Laser Desorption/Ionization: Application to Negative Ions and Further Characteristics. *Rapid Commun. Mass Spectrom.,* **12**, 529 - 534 (1998)
16. Knochenmuss, R.: MALDI Ionization Mechanisms: the Coupled Photophysical and Chemical Dynamics Model Correctly Predicts "Temperature"-Selected Spectra. *J. Mass Spectrom.,* **48**, 998-1004 (2013)
17. Knochenmuss, R.: MALDI mechanisms: wavelength and matrix dependence of the coupled photophysical and chemical dynamics model. *The Analyst,* **139**, 147-156 (2014)
18. Hoteling, A. J., Nichols, W. F., Giesen, D. J., Lenhard, J. R., Knochenmuss, R.: Electron transfer reactions in LDI and MALDI: factors influencing matrix and analyte ion intensities. *Eur. J. Mass Spectrom.,* **12**, 345-358 (2006)
19. Knochenmuss, R.: MALDI and Related Methods: A Solved Problem or Still a Mystery? *Mass Spectrom. (Japan),* **2**, S0006 (2013)
20. Knochenmuss, R., Vertes, A.: Time-delayed 2-Pulse Studies of MALDI Matrix Ionization Mechanisms. *J. Phys. Chem. B,* **104**, 5406-5410 (2000)
21. Knochenmuss, R.: Photoionization Pathways and Free Electrons in UV-MALDI. *Anal. Chem.,* **76**, 3179-3184 (2004)
22. Wallace, W. E., Arnould, M. A., Knochenmuss, R.: 2,5 dihydroxybenzoic acid: laser desorption/ionization as a function of elevated temperature. *Int. J. Mass Spectrom.,* **242**, 13-22 (2005)
23. McCombie, G., Knochenmuss, R.: Enhanced MALDI ionization efficiency at the metal-matrix interface: practical and mechanistic consequences of sample thickness and preparation method. *J.Am. Soc. Mass Spectrom.,* **17**, 737-745 (2006)
24. Knochenmuss, R.: Laser Desorption / Ablation Plumes from Capillary-Like Restricted Volumes. *Eur. J. Mass Spectrom.,* **15**, 189-198 (2009)

25. Lu, I.-C., Chu, K. Y., Lin, C.-Y., Wu, S.-Y., Dyakov, Y. A., J.-L., C., Gray-Weale, A., Lee, Y. T., Ni, C.-K.: Ion-to-Neutral Ratios and Thermal Proton Transfer in Matrix-Assisted Laser Desorption/Ionization. *J. Am. Soc. Mass Spectrom.,* (2015)
26. Liang, C. W., Lee, C. H., Lin, Y.-J., Lee, Y. T., Ni, C. K.: MALDI Mechanism of Dihydroxybenzoic Acid Isomers: Desorption of Neutral Matrix and Analyte. *J. Phys. Chem. B,* **117**, 5058-5064 (2013)
27. Lin, H.-Y., Hsu, H. C., Lu, I.-C., Hsu, K.-T., Liao, C.-Y., Lee, Y.-Y., Tseng, C.-M., Lee, Y.-T., Ni, C.-K.: Fluorescence spectroscopy of UV-MALDI matrices and implications of ionization mechanisms. *J. Chem. Phys.,* **141**, 164307 (2014)
28. Lin, H.-Y., Song, B., Lu, I.-C., Hsu, K.-T., Liao, C.-Y., Lee, Y.-Y., Tseng, C.-M., Lee, Y.-T., Ni, C.-K.: Is energy pooling necessary in ultraviolet matrix-assisted laser desorption/ionization? *Rapid Comm. Mass Spectrom.,* **28**, 77-82 (2014)
29. Setz, P., Knochenmuss, R.: Exciton Mobility and Trapping in a UV-MALDI Matrix. *J. Phys. Chem. A,* **109**, 4030-4037 (2005)
30. Hoyer, T., Tuszynski, W., Lienau, C.: Ultrafast photodimerization dynamics in alpha-cyano-4-hydroxycinnamic and sinapinic acid crystals. *Chem. Phys. Lett.,* **443**, 107-112 (2007)
31. T. Hoyer, Dr. rer. nat. Fakultät für Mathematik und Naturwissenschaften, Carl von Ossietzky Universität Oldenburg, Oldenburg (2009).
32. Lüdemann, H.-C., Redmond, R. W., Hillenkamp, F.: Singlet-singlet annihilation in ultraviolet MALDI studied by fluorescence spectroscopy. *Rapid Comm. Mass Spectrom.,* **16**, 1287-1294 (2002)
33. Liu, B.-L., Charkin, O. P., Klemenko, N., Chen, C. W., Wang, Y.-S.: Initial Ionization Reaction in Matrix-Assisted Laser Desorption/Ionization. *J. Phys. Chem. B,* **114**, 10853-10859 (2010)
34. Hoyer, T., Tuszynski, W., Lienau, C.: Competing ultrafast photoinduced quenching reactions in cinnamic acid peptide blends. *Phys. Chem. Chem. Phys.,* **12**, 13052 (2010)